ISSN 0023-1584, Kinetics and Catalysis, 2007, Vol. 48, No. 2, pp. 228–244. © MAIK "Nauka/Interperiodica" (Russia), 2007.
Original Russian Text © V.R. Khabibulin, A.V. Kulik, I.V. Oshanina, L.G. Bruk, O.N. Temkin, V.M. Nosova, Yu.A. Ustynyuk, V.K. Bel'skii, A.I. Stash, K.A. Lysenko, M.Yu. Antipin, 2007, published in Kinetika i Kataliz, 2007, Vol. 48, No. 2, pp. 244–260.

Mechanism of the Oxidative Carbonylation of Terminal Alkynes at the ≡C–H Bond in Solutions of Palladium Complexes

V. R. Khabibulin[a], A. V. Kulik[a], I. V. Oshanina[a], L. G. Bruk[a], O. N. Temkin[a], V. M. Nosova[b], Yu. A. Ustynyuk[b], V. K. Bel'skii[c], A. I. Stash[c], K. A. Lysenko[d], and M. Yu. Antipin[d]

[a] *Lomonosov State Academy of Fine Chemical Technology, Moscow, 117571 Russia*
e-mail: alkulik@gmail.com
[b] *Moscow State University, Moscow, 119899 Russia*
[c] *Karpov Research Institute of Physical Chemistry, Moscow, 103064 Russia*
[d] *Nesmeyanov Institute of Organoelement Compounds, Russian Academy of Sciences, Moscow, 117813 Russia*

Received January 11, 2006

Abstract—The formation mechanism of the active catalyst in the oxidative carbonylation of terminal alkynes at the ≡C–H bond has been investigated for the catalytic system $Pd(OAc)_2$–PPh_3–*p*-benzoquinone (Q)–MeOH. It has been demonstrated by NMR spectroscopy, X-ray crystallography, and kinetic measurements that the catalytically active palladium is in the oxidation state 0 and is bound into complexes stabilized by *p*-benzoquinone (PdL_2Q, where L = PPh_3). A mechanism is suggested for the catalytic process, which includes the formation of the complex PdL_2Q, the oxidative addition of the alkyne to this complex at the ≡C–H bond, the insertion of CO into the Pd–C bond, and steps in which hydride hydrogen is intramolecularly transferred to the *p*-quinone.

DOI: 10.1134/S0023158407020073

The oxidative carbonylations of terminal alkynes at the ≡C–H bond (I), which yield esters of arylpropiolic and alkylpropiolic acids, are of considerable theoretical and applied interest, since these esters have great synthetic potential [1].

$$\mathrm{RC{\equiv}CH + CO + MeOH + Ox} \longrightarrow \mathrm{RC{\equiv}CC(O)OMe + Red + 2H^+}. \quad \text{(I)}$$

Various oxidizers (Ox) can be used in this reaction. In the particular case of Ox = quinone, the oxidizer reduction product is Red + $2H^+$ = hydroquinone.

Comparatively selective catalytic systems for reaction (I) were reported for the first time by Tsuji et al. [2]. The most effective system is $PdCl_2$–$CuCl_2$–NaOAc, on which the following reactions proceed with 70% alkyne selectivity:

$$\mathrm{RC{\equiv}CH + CO + MeOH + 2NaOAc + 2CuCl_2} \xrightarrow{\mathrm{PdCl_2}} \mathrm{RC{\equiv}CC(O)OMe + 2NaCl + 2CuCl + 2AcOH}. \quad \text{(II)}$$

It was found earlier [3] that this catalytic system is multifunctional and reaction (II) is autocatalytic. Cu(I) chloride, which results from $CuCl_2$ reduction, is the component that catalyzes the palladium alkynyl complex formation step in mechanism (III):

$$\mathrm{RC{\equiv}CH + CuCl \xrightarrow[-HCl]{} RC{\equiv}CCu \xrightarrow[-CuCl]{PdCl_2} RC{\equiv}CPdCl}$$
$$\xrightarrow{\mathrm{CO}} \mathrm{RC{\equiv}CC(O)PdCl} \xrightarrow{\mathrm{MeOH}} \mathrm{HPdCl} \xrightarrow{\mathrm{2CuCl_2}} \mathrm{PdCl_2 + 2CuCl + HCl} \quad \text{(III)}$$
$$\mathrm{RC{\equiv}CC(O)OMe}$$

Mechanism (III) was confirmed by the synthesis and reactivity studies of Cu(I), Ag(I), and Hg(II) alkynyl complexes in reaction (II), by kinetic studies [3, 4], and by determination of the kinetic isotope effect [5]. Furthermore, these studies made it possible to carry out a new catalytic reaction using oxygen as the oxidizer and Pd(II), Cu(I), and Cu(II) as catalysts:

$$\mathrm{RC{\equiv}CH + CO + MeOH + 1/2O_2} \xrightarrow{\mathrm{PdCl_2,\ CuCl,\ CuCl_2}} \mathrm{RC{\equiv}CCOOMe + H_2O}. \quad \text{(IV)}$$

This reaction, which does not yield any acid and, therefore, does not need a base for acid neutralization, can provide a basis for small-scale production of esters of alkynylcarboxylic acids (productivity, ~40 g l^{-1} h^{-1};

Table 1. Solvent effects on MEPA synthesis in the $Pd(OAc)_2$–PPh_3–*p*-quinone–MeOH–solvent systems

p-Quinone	Solvent	Initial MEPA formation rate, mol l^{-1} h^{-1}	PA-to-MEPA conversion selectivity, %
p-Benzo-quinone	CH_3CN	0.03	51
	CH_3COCH_3	0.05	56
	$CHCl_3$	0.05	47
	1,4-dioxane	0.05	82
	THF	0.032	74
	C_6H_6	0.042	65
	CH_3OH	0.065	51
Chloranil	CH_3CN	0.054	59
	CH_3COCH_3	0.36	80
	$CHCl_3$	0.40	81
	1,4-dioxane	0.40	85
	THF	0.40	85
	CH_3OH	0.25	72

Note: $T = 31°C$, $P_{CO} = 1$ atm, [Pd] = 0.006 mol/l, [L] = 0.010 mol/l, [*p*-quinone] = 0.1 mol/l, and $[PA]_0 = 0.1$ mol/l.

desired-product selectivity, 75–85%, depending on the alkyne) [7].

For reaction (I), Tsuji et al. [2] suggested the fundamentally different catalytic system $Pd(OAc)_2$–*p*-benzoquinone (Q), which seems simpler at first glance. The subject of this publication is the mechanism of reaction (I) involving this system as the catalyst and phenylacetylene as the substrate.

PRELIMINARY EXPERIMENT: CHOOSING THE COMPOSITION OF THE CATALYTIC SYSTEM

In our preliminary experiments, we studied how the oxidative carbonylation of phenylacetylene (PA) into methyl ester of phenylpropiolic acid (MEPA) depends on the natures of the ligand, of the solvent, and of the *p*-quinone.

A *p*-quinone must be present in the $Pd(OAc)_2$–MeOH system for reaction (I) to occur. Other oxidizers, for example, Cu(II) and Fe(III) compounds, do not ensure the synthesis of MEPA. Besides *p*-benzoquinone, 2,3,5,6-tetrachloro-*p*-benzoquinore (chloranil) was tested in the synthesis. The rate and MEPA selectivity of the process were found to depend strongly on the quinone (Table 1). Therefore, the quinone plays a significant role in the process.

Phosphine admixtures, which serve as efficient ligands in the $Pd(OAc)_2$–MeOH system, cause different effects depending on their nature (Table 2). The greatest speedup of the reaction is observed with PPh_3, and this effect is stronger for the chloranyl-containing system. It is essential that PPh_3 does not decrease the selectivity of the reaction. Likewise, P(cyclo-$C_6H_{11})_3$ added to the *p*-benzoquinone-containing system speeds up the reaction significantly without causing a decrease in the selectivity. For the chloranil-containing system, P(cyclo-$C_6H_{11})_3$ affords a greater increase in the reaction rate but diminishes the selectivity of the reaction. P(*n*-$C_3H_7)_3$ exerts the opposite effect. Diphosphines

Table 2. Ligand effects on MEPA synthesis in the $Pd(OAc)_2$–*p*-quinone–MeOH systems

Quinone	Ligand	Initial MEPA formation rate, mol l^{-1} h^{-1}	PA-to-MEPA conversion selectivity, %
p-Benzoquinone	PPh_3	0.065	51
	P(*n*-$C_3H_7)_3$	0.01	44
	P(*cyclo*-$C_6H_{11})_3$	0.05	69
	PPh_2(2-Py)	0*	25
	$Ph_2PCH_2CH_2PPh_2$	0	0
	$Ph_2PCH_2CH_2CH_2PPh_2$	0	14
	o-phenanthroline	0	0
Chloranil	PPh_3	0.25	72
	P(*n*-$C_3H_7)_3$	0	82
	P(*cyclo*-$C_6H_{11})_3$	0.14	54
	PPh_2(2-Py)	0	40
	$Ph_2PCH_2CH_2CH_2PPh_2$	0	0
	o-phenanthroline	0	0

Note: $T = 31°C$, $P_{CO} = 1$ atm, [Pd] = 0.006 mol/l, [L] = 0.010 mol/l, [*p*-quinone] = 0.1 mol/l, and $[PA]_0 = 0.1$ mol/l.
* The processes with a zero initial rate have an induction period.

and nitrogen-containing ligands do not produce a favorable effect: with these ligands, PA is not converted into MEPA. Further studies were carried out with triphenylphosphine (hereafter, L = PPh_3).

The effect of the nature of the solvent on the process was again studied for the *p*-benzoquinone- and chloranil-containing systems (Table 1). In all runs involving a solvent, PA is completely converted in 1–2 h. Note again that the same solvent causes different effects in systems with different *p*-quinones. For the system containing *p*-benzoquinone, the initial reaction rate is lower in a mixed solvent (MeOH : solvent = 1 : 1 vol/vol) than in pure methanol. For the chloranil-containing system, the initial MEPA formation rate is higher in a mixed solvent than in methanol. Most solvents (except CH_3CN and $CHCl_3$ in the *p*-benzoquinone-containing system) enhance the selectivity of the process. The greatest increase in selectivity is achieved by adding 1,4-dioxane or tetrahydrofuran (THF). The strong dependence of reaction (I) on the kind of *p*-quinone and the fact that a solvent added to methanol produces different effects in systems containing different *p*-quinones suggest that the catalytically active complexes in these similar systems contain a *p*-quinone or that this *p*-quinone is involved in reaction steps preceding the rate-limiting step.

HYPOTHETIC MECHANISMS OF MEPA SYNTHESIS IN THE $Pd(OAc)_2$–PPh_3–*p*-QUINONE–MeOH SYSTEMS

When constructing hypotheses, we took into consideration the sets of mechanisms obtained by using a formalized procedure involving the ChemNet program [5, 8]. All hypothetic mechanisms can be divided into the following three groups.

(1) Mechanisms involving a key alkoxycarbonyl (methoxycarbonyl) intermediate:

$$\mathrm{PdX_2 + MeOH + CO \underset{-HX}{\rightleftharpoons} \underline{XPdC(O)OMe}}$$
$$\xrightarrow{RC\equiv CH} \mathrm{XPdC(R)=CHC(O)OMe} \xrightarrow[-HPdX]{} \mathrm{RC\equiv CC(O)OMe.} \quad (V)$$

(2) Mechanisms involving the formation of a key Pd(II) alkynyl complex at the stage of the electrophilic substitution of palladium(II) for hydrogen in the alkyne:

$$\mathrm{PdX_2 + RC\equiv CH \underset{-HX}{\rightleftharpoons} \underline{XPdC\equiv CR}}$$
$$\xrightarrow{CO} \mathrm{XPdC(O)C\equiv CR} \xrightarrow[-HPdX]{MeOH} \mathrm{RC\equiv CC(O)OMe.} \quad (VI)$$

(3) Mechanisms involving the formation of a key Pd(II) ethynyl hydrido complex at the stage of the C–H oxidative addition of the alkyne to Pd(0):

$$\mathrm{Pd(0) + RC\equiv CH \rightleftharpoons \underline{RC\equiv CPdH}}$$
$$\xrightarrow{CO} \mathrm{HPdC(O)C\equiv CR} \xrightarrow[-HPdH]{MeOH} \mathrm{RC\equiv CC(O)OMe.} \quad (VII)$$

A first-group MEPA formation mechanism was suggested by Heck [9] in 1972. No second-group mechanisms have been reported. Palladium(II) forms alkynyl complexes unreadily (much less readily than Cu(I) or Ag(I); see above). However, some Pd(II) alkynyl complexes do exist, so there is no reason to rule out the formation of such a complex by the electrophilic substitution of palladium for a hydrogen atom in the alkyne. There is only very little information concerning the possibility of the C–H oxidative addition of 1-alkynes to Pd(0) [10]. For Ni(0) and Rh(0), the possibility of this step is beyond any doubt [11].

DISCRIMINATION OF HYPOTHETICAL MECHANISMS

The above hypotheses can be verified and discriminated by experiments aimed at gaining the following information:

(1) the state of the catalyst during the oxidative carbonylation of alkynes (the oxidation state of palladium and the composition and structure of palladium complexes);

(2) the kinetic isotope effect (KIE) arising from the replacement of CH_3OH with CH_3OD or CD_3OD (if a first-group mechanism takes place, KIE will be far above unity);

(3) kinetics observed while varying the concentrations of the reactants and of the components of the catalytic system.

State of the Catalyst

The IR spectrum of the reaction solution in the mixed solvent MeOH–$CHCl_3$ changes mainly owing to MEPA bands (CO group, 1717 cm^{-1}; C≡C bond, 2200 cm^{-1}) appearing during the process.

By contrast, the changes in the ^1H and ^{31}P NMR spectra are very sophisticated. For example, some ^{31}P NMR spectra show ten to twenty time-variable phosphorus resonances. Table 3 lists the multicomponent systems studied by NMR and their designations.

In order to identify the intermediates, we investigated less complicated, model systems, including systems into which reactants were introduced one after another. NMR spectra were recorded during the reaction. Table 4 lists chemical shifts (δ) and spin–spin coupling constants (*J*) for the components of the catalytic systems and for the complexes obtained by independent synthesis.

Table 3. Multicomponent systems studied by ^{1}H, ^{13}C, and ^{31}P NMR spectroscopy

Designation	System
	Three-component
1.1	$[PPh_3–Q–CD_3OD]$, 25°C
1.2	$[PPh_3–Q–CDCl_3]$, –25°C
1.3	$[Pd(OAc)_2–Q–CD_3OD]$, 23°C
1.4	$[Pd(OAc)_2–PPh_3–CD_3OD]$, 25°C
1.5	$[Pd(OAc)_2–2PPh_3–CDCl_3]$, –25°C
1.6	$[Pd(PPh_3)_4–10Q–CDCl_3]$, –25°C
	Four-component
2.1	$[Pd(OAc)_2–PPh_3–Q–CH_3OD]$, 25°C
2.2	$[Pd(OAc)_2–PPh_3–Q–CD_3OD]$, 27°C
2.3	$[Pd(PPh_3)_4–Q–CO–CD_3OD]$, 30°C
	Five-component
3.1	$[Pd(OAc)_2–PPh_3–Q–CO–CH_3OD]$, 30°C
3.2	$[Pd(OAc)_2–PPh_3–Q–CO–CD_3OD]$, 30°C
	Six-component
4.1	$[Pd(OAc)_2–PPh_3–Q–CO–CH_3OH–CDCl_3]$, –25°C
4.2	$[Pd(PPh_3)_4–Q–CO–PhC{\equiv}CH–CH_3OH–CDCl_3]$, –25°C
	Seven-component
5.1	$[Pd(OAc)_2–PPh_3–Q–CO–PhC{\equiv}CH–CH_3OH–CDCl_3]$, –25°C
	Systems into which the reactants were introduced in sequence
6.1	$[Pd(OAc)_2–Q–CD_3OD] + [PPh_3]$, 23°C
6.2	$[Pd(OAc)_2–PPh_3–CD_3OD] + [Q]$, 23°C
6.3	$[Pd(OAc)_2–PPh_3–Q–CD_3OD] + [CO]$, 24°C
6.4	$[Pd(OAc)_2–PPh_3–CD_3OD] + [Q] + [CO]$, 26°C
6.5	$[Pd(OAc)_2–PPh_3–CD_3OD] + [Q–CO–PhC{\equiv}CH]$, 27°C
6.6	$[Pd(OAc)_2–CDCl_3] + [PPh_3] + [Q]$, –25°C
6.7	$[Pd(OAc)_2–3PPh_3–CDCl_3] + [CH_3OH] + [Q] + [CO]$, –25°C
6.8	$[PPh_3–Q–CDCl_3] + [CH_3OH] + [CO] + [PhC{\equiv}CH]$, –25°C

Note: The components that were mixed or added together are bracketed.
Q = *p*-benzoquinone.

The actual component ratios in the reactions studied by NMR were derived from total integrated intensities in the following three ^{1}H NMR spectral regions:

(1) 1–2.3 ppm, where the signals from the OAc groups of various palladium complexes and the signal from the OAc^{-} anion are observed;

(2) 7–7.9 ppm, the aromatic range accommodating the signals from the phenyl groups of triphenylphosphine, both free and coordinated to palladium in various complexes, and from the phenyl groups of the other PPh_3-containing compounds; integration in this range allows the total amount of triphenylphosphine involved in the reaction to be determined;

(3) 5.2–7.1 ppm, the range accommodating the signals from *p*-benzoquinone, hydroquinone, and all of their derivatives, including the products resulting from their interaction with PPh_3 and palladium acetate.

Palladium acetate (**I**) is known to be readily reducible with triphenylphosphine (**II**) [12]; carbon monoxide [13–16]; and, probably, methanol, all of which are present in the catalytic system. Indeed, we observed triphenylphosphine oxide (**III**) signals in nearly all reaction systems, although the amount of **III** did not exceed 4% of the amount of triphenylphosphine involved in the reaction (see below). The ^{31}P chemical shift for $O{=}PPh_3$ depends strongly on the solvent, the concentration of the compound, and temperature. The true position of the triphenylphosphine oxide signal was determined against ^{13}C satellites ($^{1}J_{P–C}$ = 102–104 Hz) in the ^{31}P NMR spectrum and from characteristic chemical shifts and constants in the ^{13}C NMR spectrum.

Table 4. ^{1}H, ^{13}C, and ^{31}P NMR data: chemical shifts (δ) and spin–spin coupling constants (*J*) ($CDCl_3$, –25°C)

Compound	Fragment	Group	^{1}H		^{13}C		^{31}P[a]
			^{1}H atom	δ, ppm, intensity, (splitting, Hz)	^{13}C atom	δ, ppm (J_{P-C} or multiplet splitting,[b] Hz)	δ, ppm ($^{1}J_{P-C}$, Hz, derived from ^{12}C satellites
I $Pd(OAc)_2$	OAc	–		2.026; 1.981[c]; 1.987[c]	–	–	–
II PPh_3	–	Ph	*ortho* *meta*, *para*	7.31–7.38 m, 2H 7.22–7.31 m, 3H	*ortho* *meta* *para* *ipso*	133.59 d (19.3) 128.44 d (6.7) 128.70 brds 136.58 d (9.4)	–6.36
III $O{=}PPh_3$	–	Ph	*ortho* *meta* *para*	7.58–7.68 m, 2H 7.42–7.49 m, 2H 7.51–7.58 m, 1H	*ortho* *meta* *para* *ipso*	131.92 d (10.6) 128.48 d (12.3) 132.04 d (2.5) 131.74 d (104.4)	30.86 (104); 33.66[d]
VI $Pd(PPh_3)_2(OAc)_2$ (yellow)	–O–C(O)–CH_3	 CH_3 C=O	*ortho* *meta*, *para*	7.65–7.73 m, 12H 7.33–7.47 m, 18H 0.806 vt, 6H, (0.51)	*ortho* *meta* *para* *ipso*	134.44 vt (6.66) 128.13 vt (5.05) 130.37 brds 128.83 vt (23.34) 21.73 vt (1.2) 175.77 s	14.92
VIII *p*-Benzoquinone	–	CH= C=O	–	6.80 s	–	136.48 187.52	–
IX Hydroquinone	–	CH= C–OH	–	6.643 s, 4H; 6.706[e] 9.00 brs, 2H	–	115.74; 116.16[e] 149.67	–
X[f] $[Pd(PPh_3)_2Q]_2$–H_2Q · MeOH (red)	–	Ph	*ortho* *meta* *para*	7.130 m, 12H 7.193 m, 12H 7.305 m, 6H	*ortho* *meta* *para* *ipso*	133.52 vt (6.83) 128.03 vt (4.94) 129.69 brds 132.15 vdd (17.2; 18.4)	31.17; 31.30[g]; 31.24[h] 33.10[d]
	–	CH= C=O		5.352 vt[i], 4H, (1.98)		104.79 t (3.2) 184.69 t (2.35)	
XI[f] $[Pd(PPh_3)Q]_2$ · 1.5MeOH (black)	–	Ph CH= CH= C=O C=O	*ortho* *meta* *para*	7.135 m, 12H 7.243 m, 12H 7.318 m, 6H 4.02 m, 4H 4.34 m, 4H	*ortho* *meta* *para* *ipso*	133.36 vt (6.47) 128.61 vt (5.05) 130.47 brds 131.99 vdd (17.2; 18.5) 78.04 t (3.69) 81.94 t (1.35) 185.61 t (3.67) 193.94 t (1.12)	16.95; 17.99[g]; 18.29[d]

Table 4. (Contd.)

Compound	Fragment	Group	^{1}H		^{13}C		^{31}P[a]
			^{1}H atom	δ, ppm, intensity, (splitting, Hz)	^{13}C atom	δ, ppm (J_{P-C} or multiplet splitting[b], Hz)	δ, ppm ($^1J_{P-C}$, Hz, derived from ^{12}C satellites
XII			*ortho*	7.63–7.72 m, 2H	*ortho*	134.86 vt (6.28)	23.88
$Pd(PPh_3)_2Cl_2$			*meta*, *para*	7.34–7.48 m, 3H	*meta*	128.03 vt (5.3)	
(yellow)	–	Ph			*para*	130.55 brds	
					ipso	128.97 vt (24.8)	
XVI			*ortho*	7.62–7.71 m, 24H	*ortho*	134.30 vt (6.58)	18.34
$[Pd(COOCH_3)$		Ph	*meta*, *para*	7.32–7.44 m, 36H	*meta*	128.15 vt (5.24)	
$(OAc)(PPh_3)_2]_2$					*para*	130.35 brds	
$H_2Q \cdot CH_3OH$					*ipso*	129.76 vt (23.04)	
	$-O-C(O)-CH_3$	CH_3		0.894 s, 6H		22.87 vt (1.1)	
		C=O				177.17 s	
	$-C(O)-OCH_3$	OCH_3		2.434 s, 6H		51.81 s	
		C=O				181.12 vt (2.3)	
	para-$(OH)_2Q$	CH=		6.624 s, 4H		115.73	
		C–OH		9.146 brds, 2H		149.71	
XVII	C≡CH	Ph	*ortho*	7.47–7.53 m, 2H	*ortho*	131.96	–
PhC≡CH			*meta*, *para*	7.30–7.38 m, 3H	*meta*	128.25	
					para	128.79	
					ipso	121.59	
PA		≡CH		3.119		77.26	
		–C≡				83.44	
XIX	–	Ph		7.4–7.63 m,	–	–	–
MEPA[g,j]		OMe		3.803			

Note: s—singlet, d—doublet, vdd—virtual doublet of doublets, t—triplet, vt—virtual triplet, brds—broadened singlet, brs—broad singlet, and m—multiplet.

[a] Measured relative to the phosphorus signal from outer 85% H_3PO_4 in H_2O.

[b] Virtual splittings are not spin–spin coupling constants, but they indicate the presence of ABX spin systems.

[c] System **6.1**, CD_5OD, 1.981 (26°C), 1.987 (23°C).

[d] CD_3OD, 27°C.

[e] $CDCl_3$, 24°C.

[f] The chemical shifts for protons are derived from $^1H\{^{31}P\}$ NMR spectra.

[g] Acetone-D_6, 25°C.

[h] $CDCl_3$, 30°C.

[i] Spin system $A_2A_2'XX'$.

[j] MEPA + ethyl benzoate (1 : 1) mixture.

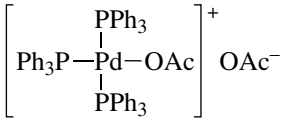

Fig. 1. Presumable structure of the complex forming in system **1.4**.

Two phosphorus signals not assignable to palladium complexes (21.7 and 16.9 ppm) appeared in the NMR spectra of all systems containing triphenylphosphine, excess *p*-benzoquinone, and methanol (Table 3, systems **2.1**–**2.3**, **3.1**, **3.2**, **6.1**–**6.5**). As was demonstrated in earlier works [17–19], the interaction between triphenylphosphine and *p*-benzoquinone is a 1,4-addition reaction yielding (2,5-dihydroxyphenyl)phosphonium betaine (**IV**); however, no NMR data for **IV** were reported in those works. We found that the main reaction product in the simplest system **1.1** (PPh_3–Q–CD_3OD, +25°C) is indeed compound **IV**, which is readily identifiable by ^1H NMR. The spectrum of **IV** exhibits signals from three nonequivalent protons at 6.13 ppm ($^4J_{HH}$= 3.18 Hz, $^5J_{HH}$ = 0.38 Hz, $^3J_{PH}$ = 15.02 Hz), 6.60 ppm ($^3J_{HH}$ = 9.04 Hz, $^5J_{HH}$ = 0.38 Hz, $^4J_{PH}$ = 7.23 Hz), and 7.01 ppm ($^3J_{HH}$ = 9.04 Hz, $^4J_{HH}$ = 3.18 Hz, $^5J_{PH}$ = 0.71 Hz). In the ^{31}P NMR spectrum of the reaction mixture, compound **IV** gives rise to a resonance at 21.7 ppm. In the reaction mixture containing excess benzoquinone, **IV** is converted into another compound (**V**), which manifests itself as a ^{31}P resonance at 16.9 ppm. The structure of **V** is being determined now.

The nature of the complexes resulting from the interaction between palladium diacetate and triphenylphosphine was found to depend strongly on the solvent and on the PPh_3 : Pd ratio.

Amatore et al. [12, 20] studied the interaction between $Pd(OAc)_2$ and a tenfold excess of PPh_3 in THF and dimethylformamide as solvents. It was demonstrated that the complex $Pd^0(PPh_3)(OAc)^-$ initially results from the reaction between $Pd(OAc)_2$ and 2 mol of PPh_3 in these solvents and that this complex reacts with excess triphenylphosphine to yield the complex $Pd^0(PPh_3)_3(OAc)^-$ (which has a pyramidal structure). It was noted that, immediately after mixing $Pd(OAc)_2$with 10 mol PPh_3 in THF, signals from the complex $Pd^{II}(PPh_3)_2(OAc)_2$ (**VI**) (14.48 ppm) and triphenylphosphine oxide are also observed in the ^{31}P NMR spectrum.

The interaction between $Pd(OAc)_2$ and PPh_3 in $CDCl_3$ at 25°C (Table 3, system **1.5**: 2 mol PPh_3; system **6.7**: 3 mol PPh_3) yields compound **VI** (70–80%, singlet at 14.92 ppm in the ^{31}P NMR spectrum).[1] A signal from triphenylphosphine oxide (1–2%, 30.98 ppm) and several weak signals from unidentified compounds (~3%) are present in the spectrum along with the signals due to **VI**. Unreacted triphenylphosphine (16–26%, –6.37 ppm) was also detected in system **6.7**. Complex **VI** was synthesized using a standard procedure [21] and was characterized by ^1H, ^{13}C, and ^{31}P NMR, so its identification based on NMR data for catalytic systems in $CDCl_3$ was not a particular problem. In the ^1H NMR spectrum of **VI**, the methyl signal of the acetoxy group (0.806 ppm) is split into a triplet because of the spin–spin coupling of the protons with the phosphorus nuclei of the two phosphine ligands ($^5J_{H–P}$ = 0.51 Hz).

In CD_3OD (system **1.4**, PPh_3: Pd ~ 3.5), the dominant complex at 23–27°C is **VII**, which likely forms from complex **VI**. The ^{31}P NMR spectrum of this system shows two broad signals (halfwidth, ~10 Hz; total amount of phosphorus nuclei, 90%), one at 30.81 ppm (triplet, 1P) and the other at 29.32 ppm (doublet, 2P), both arising from the spin system AX_2 ($J_{P–P}$ = 18.1 Hz), as well as signals from free triphenylphosphine (4.2%, broad singlet at –4.47 ppm) and triphenylphosphine oxide (3.8%, 33.66 ppm). The ^1H NMR spectrum exhibits broad and smooth signals from phenyl protons (7.08–7.55 ppm) and two signals from acetate groups (a broad one at 1.87 ppm and the other at 0.29 ppm), and the ratio of these signals is 45 : 3 : 3. These data suggest that the molecule of complex **VII** contains three phosphine ligands and two acetoxy groups, one of which is coordinated to the palladium atom.

An AX_2 spin system in the ^{31}P NMR spectrum was also observed for the planar cationic complex $[(PPh_3)_3PdH]^+$ and for the complex resulting from the interaction between palladium diacetate and triphenylphosphine in a highly polar medium (80% CF_3COOH in water) [22]. It was assumed that the latter is also a cationic complex ($[(PPh_3)_3Pd^{II}(X)]^+$ or $[(PPh_3)_3Pd^{II}(S)]^{2+}$, where X = Oac or $OCOCF_3$ and S is probably an H_2O molecule) [22]:

$$Pd(OAc)_2 + PPh_3 \xrightarrow{80\%,\ CF_3COOH\ в\ H_2O} [(PPh_3)_3Pd^{II}X]^+$$

$$\text{or } [(PPh_3)_3Pd^{II}(S)]^{2+}.$$

A planar Pd(II) complex with three triphenylphosphine ligands and one acetoxy group in the coordination sphere of palladium can also form in system **1.4**. The second OAc group is likely an anion (Fig. 1).

The signals of complex **VII** are observed in the ^1H and ^{31}P NMR spectra of systems **6.2**, **6.4**, and **6.5** immediately after mixing $Pd(OAc)_2$ with PPh_3(L : Pd = 5–8). For all four systems in methanol-D_4, complex **VII** is the dominant palladium-containing product before quinone and CO are introduced. Besides the signals of **VII**, triphenylphosphine oxide, and unreacted triphenylphosphine, two unidentified signals at 16.3 and

[1] Hereafter, when considering a compound present in the reaction mixture, we present the percentage of its phosphorus nuclei in the total number of phosphorus nuclei. From these data, one can readily derive the molar concentration of this compound in the reaction mixture.

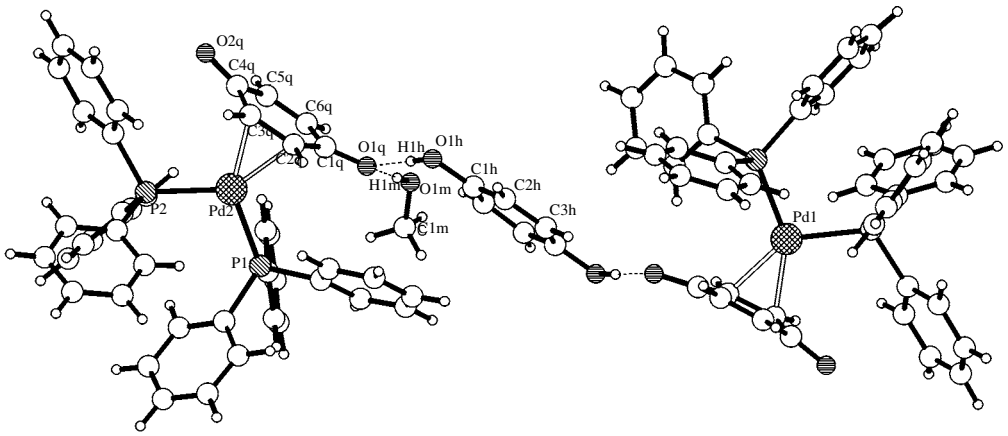

Fig. 2. Molecular structure of the complex $[Pd(PPh_3)_2Q]_2$–$H_2Q \cdot MeOH$ (**X**).

17.9 ppm (total intensity, 3%) are observed in the ^{31}P NMR spectrum. The signal at 16.3 ppm is likely due to complex **VI**.

In all the [$Pd(OAc)_2$ + PPh_3+ methanol-D_4] systems examined, including the systems containing benzoquinone and CO (**1.4**, **6.2**, **6.4**, and **6.5**), the amount of triphenylphosphine oxide does not exceed 4% of the total concentration of phosphorus-containing compounds (according to ^{31}P NMR data); therefore, triphenylphosphine is not the main Pd(II) reducer. In system **1.5**, the main product of the interaction between palladium diacetate and triphenylphosphine in $CDCl_3$ is complex **VI**. Therefore, palladium is not reduced to any significant extent because there is no nucleophile (OAc^-, MeOH, OMe^-) necessary for PR_3 oxidation with palladium.

p-Benzoquinone (**VIII**) does not form any complex with palladium diacetate in methanol (NMR data for system **1.3**, IR spectroscopic data), chloroform (IR spectroscopic data), or acetone (IR spectroscopic data). As far as we know, the literature contains no information concerning complexation between Pd(II) and *p*-benzoquinone. Only one complex between Pd(I) and *p*-benzoquinone has been reported [23], and its structure has not been determined.

Complexes between Pd(0) and *p*-benzoquinone have long been known, but hypotheses as to the structure of Pd(0)–PPh_3 compounds have been based only on indirect data [24, 25]. There is no information concerning compounds between palladium and chloranil. For identification of palladium complexes with *p*-quinones and triphenylphosphine in catalytic solutions, it was necessary to obtain, by independent synthesis, complexes that could form in the [$Pd(OAc)_2$–PPh_3–Q–MeOH] and [$Pd(PPh_3)_4$–Q–MeOH] systems. Earlier, we synthesized several palladium complexes with *p*-benzoquinone, triphenylphosphine, and *p*-hydroquinone (**IX**) and studied their structures by X-ray crystallography [26]. In the study reported here, we characterized these complexes in detail by NMR spectroscopy.

The red complex $[Pd(PPh_3)_2Q]_2$–$H_2Q \cdot MeOH$ (**X**), where H_2Q is hydroquinone (Table 4, Fig. 2), was obtained by reacting $Pd(PPh_3)_4$ with hydroquinone in a methanol solution in air at room temperature. The *p*-benzoquinone that appears in this compound results from the oxidation of *p*-hydroquinone with atmospheric oxygen. According to X-ray diffraction data, the structure of **X** is composed of two $Pd(PPh_3)_2Q$ mol-

Table 5. NMR parameters for the ABX spin systems of the phenyl carbon atoms in complex **X**

Spin system ABX				Spin–spin coupling constant, Hz		
X		A	B			
^{13}C nucleus	δ, ppm	$^{31}P(^{13}C)$, ppb	$^{31}P(^{12}C)$, ppb	$^2J_{AB}$	J_{AX}	J_{BX}
ipso	133.02	0	14 ± 2	30.45	33.95, ^1J	0.55, ^3J
	132.15*			35.1*	34.7*	0.65*
ortho	133.73	0	0	30.45	–13.5, ^2J	–0.5, ^4J
meta	128.13	0	0	30.45	9.7, ^3J	0.01, ^5J

Note: $CDCl_3$, 27°C, Bruker AM-360, 90.568 MHz.

* $CDCl_3$, –25°C, Bruker DPX-300, 75.468 MHz.

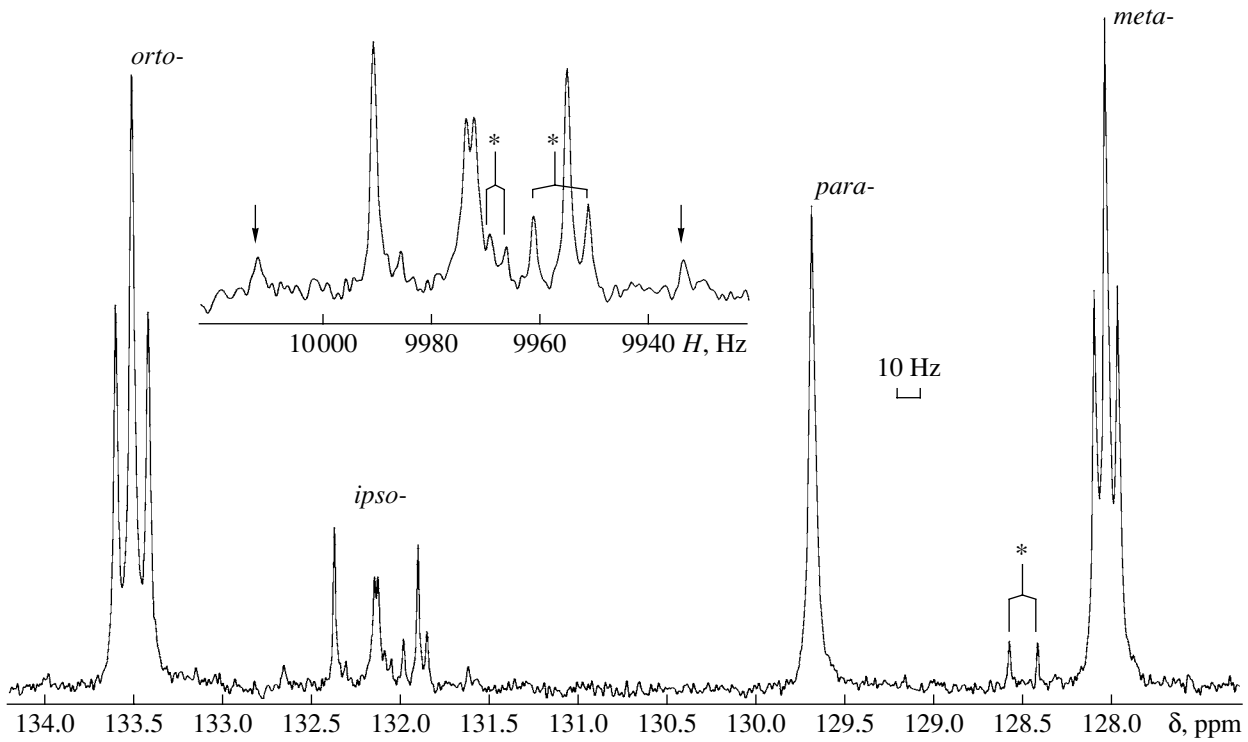

Fig. 3. ^{13}C NMR spectrum of complex **X** in the phenyl range. The signals of triphenylphosphine oxide are starred. The arrows point to the 9th and the 14th lines in the X-part of the ABX spin system of the *ipso* carbon atom.

ecules linked by a *p*-hydroquinone bridge through hydrogen bonding (Fig. 2). Pure complex **X** dissolved in $CDCl_3$ at a low temperature in an argon atmosphere gives rise to a ^{31}P resonance at 31.17 ppm (92.6%). The ^1H NMR signal of *X* occurs at 7.14–7.32 ppm. The signal from the protons of coordinated *p*-benzoquinone (A_2A_2' part of the $A_2A_2'XX'$ spin system (X, X' = ^{31}P)) is a triplet occurring at 5.35 ppm with 1.98-Hz splitting.

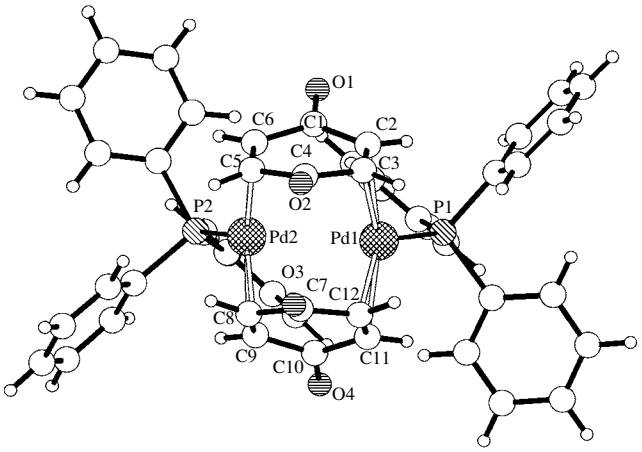

Fig. 4. Molecular structure of the complex $[Pd(PPh_3)Q]_2 \cdot 1.5MeOH$ (**XI**).

The signal intensity ratio Ph : Q = 30H : 4H is consistent with the structure of complex **X**. Furthermore, the ^1H NMR shows a *p*-hydroquinone signal at 6.58 ppm.

For **X** and other palladium complexes containing two triphenylphosphine ligands, the ^{13}C NMR spectral region pertaining to the phenyl carbon nuclei of these ligands deserves special attention (Fig. 3).

The ^{13}C NMR spectrum displays signals from all four nonequivalent types of carbon atoms, which are the X-parts of ABX spectra (A, B = ^{31}P). These spectra arise from isotopomers each containing a single ^{13}C isotope (this is possible because the natural abundance of this isotope is as low as 1.1%). As a consequence, the phosphorus atoms are nonequivalent. The $^{13}C/^{12}C$ isotope effect on ^{31}P estimated by analysis of the AB part of the spin system in the phosphorus spectrum is 14 ± 2 ppb (Table 5). The profile of the *ipso*-^{13}C multiplet is the most informative. An analysis of this multiplet allowed us to determine J_{AX} and J_{BX}. As was expected, these parameters are very different. Therefore, the profiles of the multiplets from the phenyl carbon nuclei in triphenylphosphine complexes of palladium and other transition metals provide a reliable analytical means for determining the number of phosphine ligands coordinated to the metal atom.

The dissolution of complex **X** in acetone at room temperature yields black crystals of the compound $[Pd(PPh_3)Q]_2 \cdot 1.5MeOH$ (**XI**), in which the $Pd(PPh_3)$ fragments are linked by two *p*-benzoquinone bridges (Fig. 4).

This structure of complex **XI** is confirmed by ^{1}H, ^{13}C, and ^{31}P NMR data. The ^{1}H NMR spectrum of **XI** (spin system AA'MM'XX', where X and X' are phosphorus nuclei) shows two signals with different multiplicities from the protons of the CH groups of *p*-benzoquinone coordinated to palladium. These signals occur at 4.34 ppm (4H) and 4.02 ppm (4H). Therefore, the asymmetric structure characteristic of crystals of **XI** persists in the solution. The ^{13}C NMR spectrum of **XI** shows characteristic split signals of aromatic carbon atoms, indicating that the molecule contains two triphenylphosphine ligands (see above) characterized by a spin–spin coupling constant of $J_{P...P}$ = 20–50 Hz, although these ligands are coordinated to different palladium atoms.

Complex **X** forms in a number of model systems. In system **1.6** ($Pd(PPh_3)_4$–*p*-benzoquinone (tenfold excess)–$CDCl_3$, –25°C), it accounts for ~48% of the total organophosphorus compounds content (according to ^{31}P NMR data). Furthermore, the ^{31}P NMR spectrum indicates the presence of triphenylphosphine oxide (12.4%) and of the complex $Pd(PPh_3)_2Cl_2$ (**XII**) (signal at 23.89 ppm, 6.3%) in this system. The spectrum exhibits a broad signal at 21.0 ppm (30.3%), which is likely due to the triphenylphosphine ligands in $Pd(PPh_3)_4$. The ^{31}P NMR signal of this complex in benzene occurs at 19.3 ppm. This assignment is confirmed by intensity analysis of the ^{1}H NMR signals of these compounds in the same system.

The ^{31}P NMR spectrum of the model system [$Pd(OAc)_2$–Q–PPh_3–CD_3OD], which does not contain PA or CO, shows signals from complexes **X** (systems **6.1**–**6.5**) and **XI** (systems **6.1** and **6.3**). The ^{1}H NMR spectrum of this system shows a triplet at 5.434 ppm due to complex **X** and two multiplets at 4.02 and 4.34 ppm due to complex **XI**. The concentration of the red complex **X** in methanol (CD_3OD, 25°C) is 3–14%, depending on the system. The concentration of **XI** in the methanolic solutions does not exceed 3%.

For systems **6.1**, **6.2**, and **6.4** (before passing CO), irrespective of the order in which triphenylphosphine and *p*-benzoquinone were added to $Pd(OAc)_2$ (PPh_3 : Pd = 5–8), the ^{31}P NMR spectrum shows narrow signals from three nonequivalent phosphorus nuclei forming an AMX spin system, namely, a doublet at 35.5 ppm (A), a doublet at 28.4 ppm (M), and a singlet at 23.2 ppm (X) with spin–spin coupling constants of $J(P_A–P_M)$ = 20.4 Hz, $J(P_A–P_X)$ = 1.02 Hz, and $J(P_M–P_X)$ = 0.46 Hz. The small values of J_{AX} and J_{BX} indicate the formation of a dinuclear complex containing $Pd(PPh_3)_2$ and $Pd(PPh_3)X$ fragments, where X is likely an OAc group. The signals of this complex are missing in the spectra of the similar systems **6.6** ($CDCl_3$) and **6.7** ($CDCl_3$ + CH_3OH before CO blowing) at –25°C. Apparently, under these conditions, $CDCl_3$ prevents the formation of this complex even if methanol is added to the system.

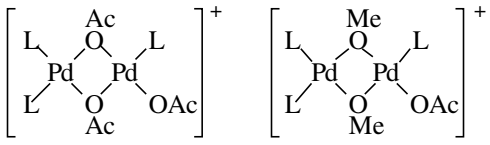

XIII **XIV**

Fig. 5. Presumable structures of the complexes forming in systems **6.1** and **6.2**.

The above results suggest that the complexes forming in systems **6.1** and **6.2** are Pd(II) complexes with structures **XIII** and **XIV** (Fig. 5).

When the reactants are combined successively (systems **6.1**, **6.2**, and **6.4**), the amount of complex **XIII** is 25–40% (as is estimated from the total integrated intensity of the signals from the three phosphine ligands). When the four reactants are combined at once (systems **2.2** and **6.3**), the amount of complex **XIII** is only 9–12%.

The above results together with relevant data reported in the literature suggest that, even before CO is introduced into the reactor, Pd(II) in the reaction solution is converted into Pd(0)–Q complexes like **X** and **XI** and into a complex like **XIII** or **XIV**.

In view of the data concerning the synthesis of complex **VI**, the sequence of reactions in the $Pd(OAc)_2$–PPh_3–Q–methanol system can be represented as follows:

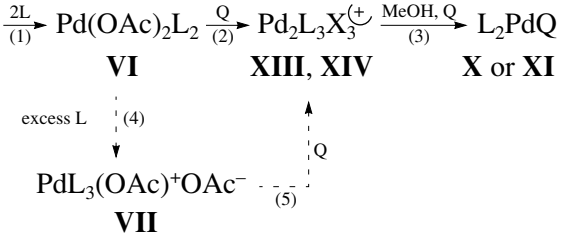

Scheme.

Dimeric, presumably Pd(II), complexes **XIII** and **XIV** coexist with Pd(0) complexes, which most likely result from the reduction of Pd(II) in the dimeric cationic complexes by methanol (reaction (3)). The

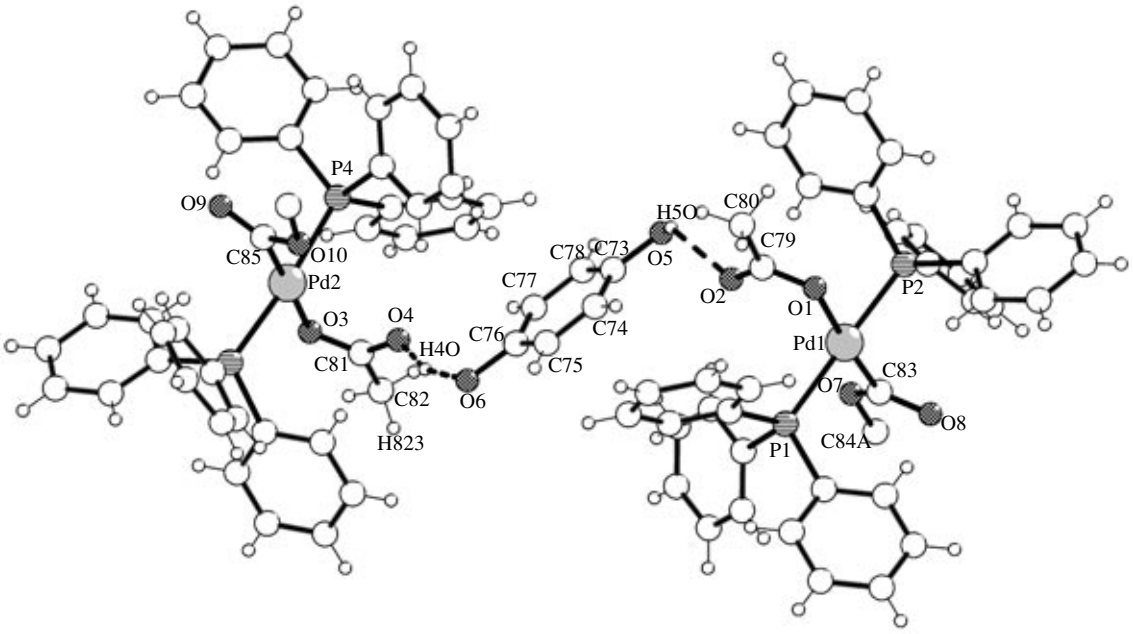

Fig. 6. Molecular structure of the complex $[Pd(COOCH_3)(OAc)(PPh_3)_2]_2H_2Q \cdot CH_3OH$ (**XVI**). The disordered methanol molecule is not shown.

quinone involved in steps (2) and (3) plays a significant role: it favors the binding of part of the PPh_3 into betaines **IV** and **V** in systems **6.1**, **6.2**, and **6.4** and the formation of the dimeric complex; as a ligand, it stabilizes Pd(0). In systems **6.1** and **6.2**, 31–51% of the PPh_3 reacts with quinone to yield betaines. Complex **VII** forms via reaction (4) in methanol, a polar solvent, in the presence of excess phosphine. It also turns into dimeric complexes upon addition of Q (scheme, reaction (5)).

The formation of palladium methoxide complexes from the cationic dimer is beyond question, since methanol is oxidized to formaldehyde and then formic acid even by palladium chloride via the formation of palladium methoxide [27].

Contrary to the reports on Pd(II) reduction with PPh_3 in THF and DMF [12, 20], PPh_3 in methanol apparently does not play any significant role in Pd(II) reduction at 25°C.

As CO is passed through the reactor (systems **6.3** and **6.4**), the signals from complexes **X** and **XI** disappear. A signal at 19.3 ppm appears in the ^{31}P NMR spectrum. The carbon signals corresponding to this signal (X-multiplets of the *ortho* and *meta* carbon atoms of ABX spin systems; see above) indicate that the new complex (**XV**) contains a $Pd(PPh_3)_2$ fragment and its composition can be, e.g., $(CO)_2Pd(PPh_3)_2$ or $(PPh_3)Pd–Pd(PPh_3)$. This complex does not contain quinone as a ligand. A Pd(0) benzoquinone complex containing no phosphine ligands presumably forms along with complex **XV**, as is indicated by a ^1H singlet at 5.34 ppm from coordinated *p*-benzoquinone. It is likely that the phosphine-free complex results from the replacement of the triphenylphosphine ligands by carbon monoxide in **X**. The amount of complex **XV** in systems **3.2**, **6.3**, and **6.4** is 14 to 60%. Complex **XV** is stable in solution. After systems **6.3** and **6.4** were stored in the cold for a short time, their ^{31}P NMR spectra indicated the same amounts of the complex.

The concentration of hydrogen ions (acid) in the systems examined is very low. The only process that can cause the acid concentration in the reaction system to exceed the acid concentration in the initial methanolic solution is palladium reduction involving PPh_3 and methanol, CO and H_2O, or CO and methanol, for example,

$$Pd(OAc)_2 + CO + 2MeOH \longrightarrow Pd(0) + O{=}C(OMe)_2 + 2AcOH. \quad \text{(VIII)}$$

The mechanism of reaction (VIII) includes the formation of an intermediate methoxycarbonyl complex, whose decomposition yields dimethyl carbonate and Pd(0) [15, 16, 28]. The methoxycarbonyl complex can also be an intermediate in the process examined (see the first-group hypotheses). The dimeric methoxycarbonyl complex $[Pd(COOMe)(OAc)(PPh_3)_2]_2C_6H_4(OH)_2$ (**XVI**) was isolated from the $Pd(OAc)_2–PPh_3–Q–MeOH$ system treated with CO (Fig. 6; see Experimental).

The compound **XVI** was characterized by X-ray crystallography and ^1H, ^{13}C, and ^{31}P NMR spectroscopy. The ^1H NMR spectrum of **XVI** (Table 4) shows signals from *p*-hydroquinone (6.624 ppm, 4H, CH=; 9.146 ppm, 2H, OH). As deduced from the integrated

Table 6. Effects of acid and base admixtures on the parameters of reaction (I) with the catalytic system $Pd(OAc)_2$–PPh_3–Q–MeOH

*n**	pH	Initial MEPA formation rate, mol l^{-1} h^{-1}	PA-to-MEPA conversion selectivity, %
Reference system			
–	6.0	0.07	51
Admixture of CH_3COOH			
1	6.0	0.12	47
2	5.9	0.10	45
3	6.0	0.08	46
Admixture of CF_3COOH			
2	0.4	0.00	0
Admixture of CH_3COONa			
1	7.0	0.07	55
2	7.3	0.12	53
4	7.5	0.13	61
6	7.7	0.10	59
10	7.7	0.09	62

* Number of moles of an acid or a base per mole of Pd(II) at $[PPh_3] : [Pd]_\Sigma = 2$.

line intensities in the proton spectrum, the complex contains two acetoxy groups (0.894 ppm, 6H) and four triphenylphosphine ligands (7.62–7.71 ppm, 24H, *ortho* protons; 7.32–7.44 ppm, 36H, *meta* and *p* protons) per *p*-hydroquinone molecule. The ^{13}C NMR spectrum of **XVI** exhibits signals from all these functional groups, and their intensities are consistent with the proton spectrum.

According to X-ray structure determination data (Fig. 6; see Experimental), complex **XVI** is a dimer in which two $Pd(COOMe)(OAc)(PPh_3)_2$ fragments are *p*-hydroquinone-bridged through hydrogen bonds between the hydroxyl hydrogen atoms of *p*-hydroquinone and the oxygen atoms of the acetate groups.

Thus, CO brings about the formation of complex **XVI** and its decomposition in the presence of a *p*-quinone—another route for the formation of Pd(0) complexes:

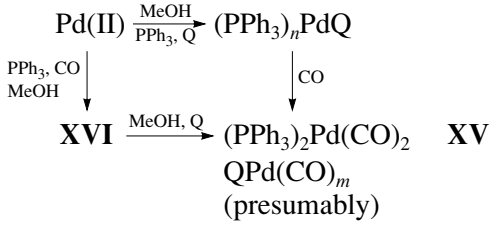

Likely Mechanisms of Reaction (I) (Ox = O)

The concentration of hydrogen ions in the system and its effect on the parameters of the process are the major discriminating factors governing the possibility of Pd(0) oxidation by a *p*-quinone (the oxidation potential of *p*-quinones decreases greatly as pH is raised to 5–6) and the realizability of first- and second-group hypotheses. pH measurements during the processes demonstrated that, at the early stages of the reaction, the solution acidity does not rise and pH remains invariable (~6). Investigation of the effects of acetic acid and sodium acetate admixtures on the pH value of the reaction solution and on the process parameters demonstrated that the system as a whole has the properties of a buffer and all its components can react with acetic acid (Table 6). The pH of the system remains almost invariable as 1 to 4 mol of CH_3COOH per mole of palladium is added. The process parameters also vary only slightly (Table 6). Only addition of 2 mol of the strong acid CF_3COOH per mole of palladium reduces pH to 0.4 and completely terminates the carbonylation reaction. These data are consistent with the third-group mechanisms, since the acetic acid resulting from palladium(II) acetate reduction is neutralized through reactions with the components of the catalytic system.

Likewise, adding up to 10 mol of a base (CH_3COONa) per mole of palladium causes only slight changes in pH and in the initial rate and selectivity of the process (Table 6). As pH is changed from 6 to 7.7, the process parameters do not change significantly. These results are most consistent with the third-group

Table 7. Effect of the nature of the initial palladium compound on the parameters of reaction (I)

Catalyst precursor	Quasi-steady-state reaction rate, mol l^{-1} h^{-1}	Reaction time, min	PA-to-MEPA conversion selectivity, %
$Pd(PPh_3)_2Cl_2$	0.000	120	Traces
$Pd(OAc)_2 + 2PPh_3$	0.043	200	58
$Pd(PPh_3)_4$	0.070	127	54
$[Pd(PPh_3)_2Q]_2H_2Q \cdot MeOH$	0.080	104	63
$[Pd(PPh_3)Q]_2 \cdot 1.5MeOH + 2PPh_3$	0.042	184	68
$Pd(dba)_2 + 2PPh_3$	0.031	219	72

Note: $T = 31°C$, $P_{CO} = 1$ ata, [Pd] = 0.006 mol/l, $[PA]_0 = 0.1$ mol/l, [Q] : [Pd] = 17.
dba = dibenzylideneacetone.

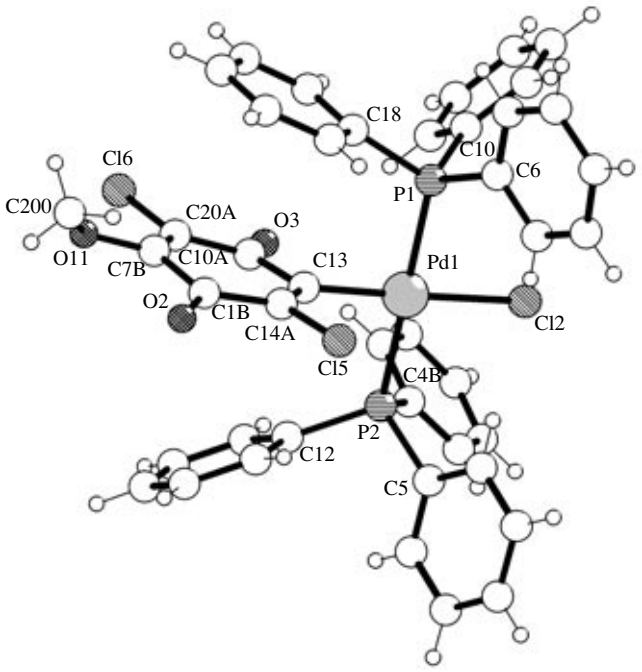

Fig. 7. Molecular structure of the complex $(PPh_3)_2ClPdC_6Cl_2O_2(OMe)$ (**XVIII**).The solvate molecule of 2,5-dichloro-3,6-dimethoxy-1,4-benzoquinone is not shown.

mechanisms, since the first- and second-group mechanisms imply that the reaction rate depends significantly on the proton concentration (they involve reversible and, probably, quasi-equilibrium steps in which H^+ is released). The termination of the process by CF_3COOH in a third-group mechanism can be caused by the decomposition of the palladium alkynyl complex resulting from the oxidative addition of the alkyne to Pd(0) at the C–H bond.

It is possible that the weak dependence of the process parameters on the acidity of the reaction solution is evidence that the *p*-quinone protonation step does not play any significant role in the oxidation of the reduced form of the catalyst. Therefore, the *p*-quinone does not oxidize Pd(0) in the process examined. The presence of complex **X** (48%) in the $Pd(PPh_3)_4$–10Q–$CDCl_3$ solution (system **1.6**) is further evidence that excess *p*-quinone does not cause Pd(0) oxidation, apparently because of the nearly complete absence of hydrogen ions.

Table 8. MEPA formation rates in the system $Pd(OAc)_2$–chloranil–PPh_3–CH_3OH/CH_3OD–chloroform (95%)

Alcohol	Reaction rate, mol l^{-1} h^{-1}	Average	Standard deviation
CH_3OH	0.25	0.22	±0.02
	0.21		
	0.21		
	0.20		
CH_3OD	0.17	0.19	±0.01
	0.20		
	0.19		
	0.20		

Comparing the catalytic activities of the initial compounds (precursors) containing Pd(II) or Pd(0) suggests that the compounds tested show similar catalytic properties in reaction (I) (Table 7). The most plausible explanation for this fact is that all precursors but $Pd(PPh_3)_2Cl_2$ turn into the same or similar compounds. These compounds are most likely Pd(0) *p*-quinone complexes containing a PdL_nQ fragment. Since reducing agents (CO, MeOH, PPh_3) are present in the system and the *p*-quinones have a low oxidation potential, the reduction of Pd(II) to Pd(0) is much more probable than the reverse process.

The above results suggest that the third-group mechanisms are the most likely. We have not detected any hydrido complexes of palladium in the catalytic solution. It is possible that, after phenylacetylene (**XVII**) is coordinated to palladium, its proton is rapidly transferred intramolecularly to the quinone coordinated to the same metal atom, involving or not involving an intermediate hydride, to yield the alkynyl–*p*-hydroquinolate palladium(II) derivative $Pd(O–C_6H_4OH)(C{\equiv}CPh)$.

The complex $(PPh_3)_2ClPdC_6Cl_2O_2(OMe)$ (**XVIII**), which was isolated from the $Pd(OAc)_2$–PPh_3–MeOH–CO–chloranil system, provides further evidence that Pd(0) is present in the reaction system examined. The most likely route for the formation of **XVIII** is the oxidative addition of chloranil to the Pd(0) complex at the C–Cl bond followed by the substitution of a methoxy group for a chlorine atom in the chloranil molecule. The composition and structure of the $(PPh_3)_2ClPdC_6Cl_2O_2(OMe)$ complex were determined by X-ray crystallography (Fig. 7; see Experimental).

As was noted above, the first-group hypotheses can be checked by KIE measurements. The kinetic experiments carried out for the $Pd(OAc)_2$–PPh_3–chloranil–CH_3OH (CH_3OD)–chloroform (95%) system demonstrated that $KIE_{H/D}$ is close to unity (Table 8). This result rules out the first-group hypotheses.

The totality of our data allow us to exclude from consideration the hypotheses involving a Pd(II) compound as an active species, the steps involving protons, and Pd(0) reoxidation with *p*-benzoquinone (because of the insufficient proton concentration) and to suggest a reaction mechanism consistent with the third-group hypotheses.

The following two schemes of the catalytic cycle can be suggested:

(1) Hydridoalkynyl mechanism (Fig. 8, outer cycle).

PA adds oxidatively to the Pd(0)–PdL_2Q intermediate to yield an organopalladium hydride for which two

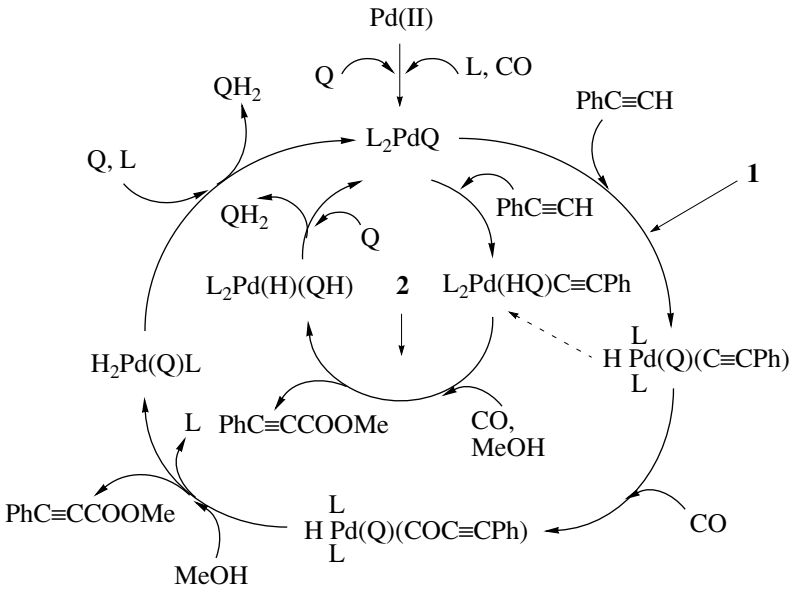

Fig. 8. MEPA synthesis mechanism including the oxidative addition of PA to Pd(0) at the ≡C–H bond. Q = *p*-quinone and L = PPh_3.

further conversion pathways are possible, namely, the oxidation of the hydrido ligand by the *p*-quinone, yielding palladium hydroquinolate (Fig. 8, mechanism 2), and the insertion of carbon monoxide into the palladium–alkynyl σ-bond. The alcoholysis of the Pd–C(O) bond in the propioloyl derivative of palladium results in the decomposition of the organopalladium intermediate into molecules of the product (MEPA, **XIX**) and the dihydrido *p*-quinone complex (Q)$LPdH_2$. The hydrido ligands are oxidized by the coordinated *p*-quinone molecule, and the phosphine ligands and *p*-quinone present in the system ensure the regeneration of the L_2PdQ complex.

(2) Hydroquinolate–alkynyl mechanism (Fig. 8, inner cycle).

Mechanism 2 does not imply the formation of a hydrido complex from PA. In this mechanism, the proton of the coordinated alkyne is intramolecularly transferred to the coordinated *p*-quinone molecule, resulting in Pd(0) oxidation and the formation of a hydroquinolate derivative. This is followed by CO insertion into the Pd–alkynyl σ-bond and, next, the alcoholysis of the Pd–C(O) bond yielding a molecule of the product (MEPA) and the hydroquinolate complex $L_2(HQ)PdH$. The complex $L_2(HQ)PdH$ is reduced to L_2Pd^0 via the reductive elimination of *p*-hydroquinone, and the latter complex reacts with *p*-quinone to turn into L_2PdQ.

Both mechanisms are in agreement with our data, and discrimination between them will be the subject of forthcoming studies.

Our data concerning the oxidative carbonylation of PA suggest that the reaction system possesses the properties of a buffer at pH 6–7.7. The findings that $KIE_{H/D} \approx 1$ is close to unity and that the initial system based on $Pd(OAc)_2$ and the complexes PdL_n, **X**, and **XI** show similar catalytic activities are evidence that L_nPdQ or $(CO)_mPdQ$ palladium(0) complexes participate in reaction (I) as catalysts. The role of *p*-quinone in this system is not only to oxidize the hydrido complexes of palladium. It is likely that *p*-quinone is involved in the reaction steps yielding the active Pd(0) complex and, as a ligand, in the alkyne activation step, followed by the intramolecular transfer of hydride hydrogen or a proton from the alkyne to the oxygen atoms of coordinated Q.

EXPERIMENTAL

The PA and MEPA concentrations in catalytic solutions were determined using an LKhM-80 gas chromatograph (thermal-conductivity detector; column packed with Porapak P, l = 1 m, d = 3 mm; carrier gas, helium; column, injector, and detector temperatures, 230, 250, and 240°C, respectively). Isobutyl benzoate or ethyl benzoate was used as the standard. The gas in contact with the solution was analyzed on an LKhM-8MD gas chromatograph (thermal-conductivity detector; column with activated carbon AR-3, l = 3 m, d = 3 mm; carrier gas, argon; column and detector temperature, 160°C; injector temperature, 200°C).

Infrared spectra were recorded on a Specord M82 spectrophotometer.

The ^1H, $^1H\{^{31}P\}$, $^{13}C\{^1H\}$, and $^{31}P\{^1H\}$ NMR spectra of compounds **I**–**XIX** in $CDCl_3$ (–25°C) were obtained on a Bruker DPX 300 spectrometer operating at 300.13, 75.468, and 121.495 MHz, respectively. Chemical shifts for phosphorus nuclei were measured relative to the signal from external 85% H_3PO_4 in H_2O. Reactions were carried out in an Ar or N_2 atmosphere.

Table 9. Crystal data and X-ray structure determination parameters for complex **XVI**

Formula	$C_{87}H_{80}O_{11}P_4Pd_2$
Molecular weight	1638.19
System	Triclinic
Space group	*P*-1
a, Å	10.594(2)
b, Å	14.119(3)
c, Å	26.705(5)
α, deg	85.57(3)
β, deg	89.40(3)
γ, deg	76.82(3)
V, Å^3	3877.5(13)
Z	2
d_{calc}, g/cm^3	1.403
μ, cm^{-1}	0.607
Total number of reflections measured (R_{int})	14428 (R_{int} = 0.0208)
Number of reflections with $I > 2\sigma(I)$	5922
Number of refined parameters	775
*R*1 ($I > 2\sigma(I)$)	0.0677
*wR*2 (for all reflections)	0.1831

Kinetic experiments were carried out in a closed, thermostated glass reactor fitted with a precessing mechanical stirrer. The weighed components of the catalytic system were charged into the reactor, and methanol and, if necessary, another solvent were added. The reactor was thermostated, carbon monoxide was passed through the reaction system, and phenylacetylene was injected using a microsyringe. During the reaction, we measured the volume of the gas consumed and sampled the gas and the solution for GC analysis.

Synthesis of complex XVI. A mixture of $Pd(OAc)_2$ (0.15 mmol) and PPh_3 (0.31 mmol) in methanol (4 ml) was stirred for 5 min. This resulted in a light green precipitate. *p*-Benzoquinone (0.573 mmol) was added to the precipitate, and CO was passed through the mixture for 10–15 min while stirring. This yielded a light yellow solution. The solution was filtered, and hexane (0.5 ml) was added. The resulting solution was cooled to +5°C. Yellow crystals formed in 48 h.

Synthesis of complex XVIII. A mixture of $Pd(OAc)_2$ (0.114 mmol) and PPh_3 (0.23 mmol) in methanol (4 ml) was stirred for 5 min. This resulted in a light green precipitate. CO was passed through the system for ~10–15 min while stirring. This yielded a homogeneous light yellow solution. Chloranil (0.55 mmol) was added to the solution. The resulting solution was stirred for 15–20 min and was then cooled to +5°C. Yellow crystals resulted in 2 months.

X-ray structure determination of complexes XVI and XVIII. The X-ray diffraction experiment for $[Pd(COOCH_3)(OAc)(PPh_3)_2]_2H_2Q \cdot CH_3OH$ (**XVI**) was carried out on a CAD-4 automated diffractometer (β-filter, λMo – K_α, λ = 0.71073 Å, *T* = 293(2) K, θ/2θ scan mode). The crystal disintegrated slowly during the experiment, and this caused a 36% change in the reference reflection intensities.

The intensity losses caused by crystal breakdown were compensated for by recovering integrated intensities from reflection profiles [29]. Crystal data and the structure determination parameters for complex **XVI** are presented in Table 9.

The structure was solved by direct methods using the SHELXS97 program [30] and was refined using the SHELXL program [31]. The positions and thermal parameters of the non-hydrogen atoms were refined isotropically and then anisotropically using full-matrix least squares. The hydrogen atoms were placed in their geometrically calculated positions and were included in the refinement in the riding model.

In the dimeric noncentrosymmetric complex, two metal complex fragments of composition $Pd(C(O)OCH_3)(OAc)(PPh_3)_2$ are linked by a hydroquinone bridge (Fig. 6). *p*-Hydroquinone is hydrogen-bonded with the carbonyl oxygen atoms of the acetate groups coordinated to the metal atom. The distances between oxygen atoms involved in hydrogen bonding are similar (O5–O2 2.679(4) Å, O4–O6 2.632(4) Å). At the same time, H–O–H angles differ significantly (O4–H40–O6 157.15(1)°, O2–H50–O5 129.95(2)°). Note that one proton of *p*-hydroquinone (H40) is nearly completely shared between an oxygen atom of *p*-hydroquinone (H40–O4 1.260(1) Å) and an oxygen atom of the acetate group (H40–O6, 1.425(2) Å). This is not the case for the other hydrogen bond (O5–H50 0.674(1) Å, O2–H50 2.195(2) Å). However, the sharing of the proton exerts only a slight effect on the C–O bond length in *p*-hydroquinone (in the case of proton sharing, C76–O6 1.375(1) Å; in the case of the normal hydrogen bond, C73–O5 1.366(1) Å) and a stronger effect on the C=O bond of the acetate ligand. The length of this bond is 1.275(2) Å in the ligand that shares the proton and 1.245(2) Å in the ligand that does not share the proton.

In the aromatic ring of the bridging *p*-hydroquinone molecule, all C–C bond lengths are between 1.389 and 1.391 Å, within the range typical of aromatic rings. The metal atom is in a square-planar coordination environment, which is typical of Pd(II) complexes. The phosphine ligands are *trans*, and the Pd–P bond lengths lie in the range 2.327(4)–2.236(4) Å. The aceto group is coordinated to Pd through one oxygen atom, and the O3–Pd2 bond length is 2.085(8) Å. The methoxycarbonyl group is *trans* to the aceto group, and the length of the Pd2–C85 σ-bond is 1.966(2) Å. The angles between the Pd–C bond and the carbonyl and ester oxygen atoms are O9–C85–Pd2 125.2(1)° and O10–C85–Pd2 113.4(1)°, respectively. In one of the two metal com-

Table 10. Crystal data and X-ray structure determination parameters for complex **XVIII**

Formula	$C_{47}H_{33}Cl_4O_5P_2Pd$
Molecular weight	987.87
System	Monoclinic
Space group	$P2(1)/c$
a, Å	12.382(2)
b, Å	10.745(19)
c, Å	32.206(6)
α, deg	90.00
β, deg	92.770(5)
γ, deg	90.00 (3)
V, Å^3	4279.6(13)
Z	4
d_{calc}, g/cm^3	1.533
μ, cm^{-1}	0.805
Total number of reflections measured (R_{int})	34 176 (R_{int} = 0.0948)
Number of reflections with $I > 2\sigma(I)$	3905
Number of refined parameters	531
$R1$ ($I > 2\sigma(I)$)	0.0645
$wR2$ (for all reflections)	0.1484

Table 11. Selected bond lengths (d) and bond angles (ω) for **XVIII**

Bond	d, Å	Angle	ω, deg
Pd1–P2	2.307(2)	C7B–O11–C200	120.4(110)
Pd1–P1	2.314(2)	P2–Pd1–P1	175.55(7)
Pd1–Cl2	2.361(2)	P2–Pd1–Cl2	88.54(7)
P2–C12	1.809(7)	C13–Pd1–Cl2	177.8(2)
P2–C5	1.814(7)	P2–Pd1–Cl2	88.54(7)
P2–C4B	1.822(7)		

plex fragments, the coordinated methoxycarbonyl group is partially disordered. A heavily disordered methanol molecule is also present in the crystal structure.

Comparing this structure with the structure of *trans*-acetatomethoxycarbonyl(bistriphenylphosphine)palladium [32], which has no *p*-hydroquinone bridge, suggests that the most important structural features of the metal complex moiety, the mutual arrangement and the coordination modes of the ligands, the geometry of the environment of the metal atom, and the bond lengths and bond angles are invariable and are independent of the synthetic route, the crystallization procedure, and the presence of a supramolecular environment.

The most significant structural distinction between the metal complex moieties is that the C=O bond lengths in their acetate ligands differ by 0.044 Å. The greatest bond angle difference is 2.7°, which is observed for the angle between the Pd–C bond and the C–O–C bond in the methoxycarbonyl ligand.

X-ray structure determination for the complex $(PPh_3)_2ClPdC_6Cl_2O_2(OMe)$ (**XVIII**) was carried out according to a standard procedure [33] on a Bruker AXS SMART 100 diffractometer fitted with a CCD detector (λMo; graphite monochromator; 110 K; ω-scan mode; $2\theta_{max} = 60°$; 0.3° increments; frame measurement time, 15 s). The structure was solved by direct methods using the SHELXS97 program [30] and was refined by anisotropic full-matrix least squares using the SHELXL97 program [31] (the H atoms were located geometrically and were fixed in their positions with $U_H = 0.08$ Å^2). Crystal data and structure determination parameters for complex **XVIII** are presented in Table 10.

According to X-ray diffraction data, **XVIII** (Tables 10, 11) is a tetracoordinated palladium(II) complex. The metal atom is in a square-planar coordination environment, which is typical of Pd(II) complexes. The coordination sphere of the metal atom consists of two *trans* triphenylphosphine ligands, a chlorine atom, and 2,5-dichloro-3-methoxy-1,4-benzoquinonyl in the *trans* position relative to the chlorine atom. The average plane of the 2,5-dichloro-3-methoxy-1,4-benzoquinonyl ring and the plane passing through the phosphorus and chlorine atoms bonded to palladium make an angle close to 90°. The methyl fragment of the methoxy group of 2,5-dichloro-3-methoxy-1,4-benzoquinonyl is partially disordered. The C–C bonds in coordinated 2,5-dichloro-3-methoxy-1,4-benzoquinonyl have lengths usual for the *p*-hydroquinone series. The double bonds are C20A–C7B 1.317(1) Å and C14A–C13 1.323(1) Å. The lengths of the ordinary bonds are between C13–C10A 1.521(1) Å and C20–C10 1.490(1) Å. The length of the Pd1–C13 σ-bond is 1.996(8) Å.

ACKNOWLEDGMENTS

This work was supported by the Russian Foundation for Basic Research, grant nos. 01-03-32883, 04-03-33014, 05-03-08134, and 05-03-33151.

REFERENCES

1. Yashina, O.G. and Vereshchagin, L.I., *Usp. Khim.*, 1978, vol. 47, p. 557.
2. Tsuji, J., Takahashi, M., and Takahashi, T., *Tetrahedron Lett.*, 1980, vol. 21, no. 9, p. 849.
3. Zung, T.T., Bruk, L.G., and Temkin, O.N., *Mendeleev Commun.*, 1994, no. 2, p. 2.
4. Zung, T.T., Bruk, L.G., and Temkin, O.N., *Izv. Akad. Nauk, Ser. Khim.*, 1993, no. 42, p. 1730.

5. Bruk, L.G., Gorodsky, S.N., Valdes-Perez, R.E., and Temkin, O.N., *J. Mol. Catal. A: Chem.*, 1998, no. 130, p. 29.
6. Bruk, L.G. and Temkin, O.N., *Inorg. Chim. Acta*, 1998, vol. 280, p. 202.
7. RF Patent 2051896.
8. Shalgunov, S.I., Zeigarnik, A.V., Bruk, L.G., and Temkin, O.N., *Izv. Akad. Nauk, Ser. Khim.*, 1999, no. 10, p. 1891.
9. Heck, R.F., *J. Am. Chem. Soc.*, 1972, vol. 94, no. 8, p. 2712.
10. Chukhadzhyan, G.A., Evoyan, Z.K., and Melkonyan, L.N., *Zh. Obshch. Khim.*, 1975, vol. 45, p. 1114.
11. Nesmeyanov, A.N. and Kocheshkov, K.A., *Metody elementoorganicheskoi khimii* (Methods of Organoelement Chemistry), Moscow: Nauka, 1978.
12. Amatore, C., Carre, E., Jutand, A., and M'Barki, M.A., *Organometallics*, 1995, vol. 14, no. 4, p. 1818.
13. Moiseev, I.I., Stromnova, T.A., Vargaftik, M.N., Mazo, G.Ja., Kuz'mina, L.G., and Struchkov, Y.T., *J. Chem. Soc., Chem. Commun.*, 1978, p. 27.
14. Chernysheva, T.V., Stromnova, T.V., Vargaftik, M.N, and Moiseev, I.I., *Izv. Akad. Nauk, Ser. Khim.*, 1996, no. 10, p. 2456.
15. Rivetti, F. and Romano, U., *J. Organomet. Chem.*, 1978, vol. 154, p. 323.
16. Rivetti, F. and Romano, U., *J. Organomet. Chem.*, 1979, vol. 174, p. 221.
17. Arshad, M., Beg, A., and Siddiqui, M.S., *Tetrahedron*, 1966, vol. 22, no. 7, p. 2203.
18. Ramirez, F. and Dershowitz, S., *J. Am. Chem. Soc.*, 1956, vol. 78, p. 5614.
19. Kutyrev, A.A. and Moskva, V.V., *Usp. Khim.*, 1987, vol. 56, no. 11.
20. Amatore, C. and Jutand, A., *Acc. Chem. Res.*, 2000, vol. 33, p. 314.
21. Dzhemilev, U.M., Popod'ko, N.R., and Kozlova, E.V., *Metallokompleksnyi kataliz v organicheskom sinteze: alitsiklicheskie soedineniya* (Metal Complex Catalysis in Organic Synthesis: Alicyclic Compounds), Moscow: Khimiya, 1999.
22. Zudin, V.N., Chinakov, V.D., Nekipelov, V.M., Rogov, V.A., Likholobov, V.A., and Yermakov, Yu.I., *J. Mol. Catal. A: Chem.*, 1989, no. 52, p. 27.
23. Shitova, N.B., Kuznetsova, L.N., Yurchenko, E.N., Ovsyannikova, I.A., and Matveev, K.I., *Izv. Akad. Nauk SSSR, Ser. Khim.,* 1973.
24. Takahashi, S. and Hagihara, N., *J. Chem. Soc. Jpn., Pure Chem. Sect.*, 1967, no. 88, p. 1306.
25. Milani, B., Anzilutti, A., Vicentini, L., Sessanta o Santi, A., Zangrando, E., Geremia, S., and Mestroni, G., *Organometallics*, 1997, no. 16, p. 5064.
26. Kulik, A.V., Bruk, L.G., Temkin, O.N., Khabibulin, V.R., Belsky, V.K., and Zavodnik, V.E., *Mendeleev Commun.*, 2002, p. 47.
27. Moiseev, I.I., *π-Kompleksy v zhidkofaznom okislenii olefinov* (π-Complexes in Liquid-Phase Alkene Oxidation), Moscow: Nauka, 1970.
28. Zhir-Lebed', L.N., Kuz'mina, L.G., Struchkov, Yu.T., Temkin, O.N., and Golodov, V.A., *Koord. Khim.*, 1978, vol. 4, p. 1046.
29. Strel'tsov, V.A. and Zavodnik, V.E., *Kristallografiya*, 1989, vol. 34, no. 6, p. 1369.
30. Sheldrick, G.M., *SHELXS97: Program for the Solution of Crystal Structures*, Göttingen: Univ. of Göttingen, 1997.
31. Sheldrick, G.M., *SHELXL97: Program for Refinement of Crystal Structures*, Göttingen: Univ. of Göttingen, 1997.
32. Del Piero, G. and Cesari, M., *Acta Crystallogr., Sect. B*, 1979, no. 35, p. 2411.
33. *SMART (Control) and SAINT (Integration) Software, Version 5.0*, Madison, WI: Bruker AXS, 1997.